Many-body effects in highly acceptor-doped GaAs/$Al_xGa_{1-x}As$ quantum wells

P. O. Holtz, A. C. Ferreira, B. E. Sernelius, A. Buyanov, and B. Monemar
Department of Physics and Measurements Technology, Linköping University, S-581 83 Linköping, Sweden

O. Mauritz and U. Ekenberg
Department of Physics, Royal Institute of Technology, S-100 44 Stockholm, Sweden

M. Sundaram, K. Campman, J. L. Merz, and A. C. Gossard
Center for Quantized Electronic Structures (QUEST), University of California at Santa Barbara, Santa Barbara, California 93016

(Received 12 November 1997)

The optical properties of quantum wells, which are center-doped with acceptors up to the high doping regime, 1×10^{19} cm^{-3}, have been studied by means of photoluminescence and photoluminescence excitation spectroscopy. The experimental results derived from the optical measurements are compared with theoretical predictions on the self-energy shifts of the subbands at high doping levels performed with self-consistent Hartree calculations with the inclusion of many-body effects. [S0163-1829(98)07432-3]

I. INTRODUCTION

The free-exciton (FE) states in a semiconductor are formed from the free-particle states of the conduction and valence bands. In a heavily doped semiconductor the presence of a large number of carriers strongly affects the exciton properties.[1] In bulk semiconductors the screening may be strong enough to inhibit the exciton formation. Thus there is an upper limit of free-carrier density, above which the excitons do not survive. In bulk GaAs, excitons are quenched already at doping levels around 10^{16} cm^{-3}, which is well below the metallic limit.[2] In *n*-type GaAs/$Al_xGa_{1-x}As$ quantum well (QW) structures, on the other hand, excitons are found to survive all the way up to the degenerate limit, due to the inefficiency of screening in a two-dimensional (2D) system.[3] In this work, we have highlighted the topic of survival of excitons at and above the degenerate limit in *p*-type GaAs/$Al_xGa_{1-x}As$ QW's. There is an additional effect from the presence of the free carriers to take into account, viz., the shifts of the electron and hole states induced by many-body interactions. We make the basic assumption that the many-body shifts characterizing the free carriers survive when the excitons are formed, i.e., we assume that the exciton energy attains a many-body shift equal to the sum of the energy shifts of the free-electron and -hole states from which the exciton is formed. The screening and the many-body shifts have opposing effects on the exciton energy.[4] In our treatment we neglect the effect of screening of the electron-hole interaction.

In the photoluminescence (PL) experiment, the electrons are excited across the band gap. Exciton states can be formed from the free-particle states at the band extrema. At low or moderate doping levels, only excitons originating from electrons (e) at the bottom of the conduction band and heavy holes (hh's) at the top of the valence band are formed at low temperatures. In the PL excitation (PLE) experiment, there must be unoccupied free-hole and free-electron states available for the formation of excitons. The excitons are assumed to be formed by electrons and holes with the same momentum. Accordingly, in the case of excitation of the *e*-hh excitons at low temperature in highly acceptor doped QW's, excitons are formed by electrons and holes with the momentum characterizing the heavy-hole states at the Fermi edge. The band-filling effect consequently gives rise to a blueshift in PLE compared to the peaks in PL, in addition to the usual Stoke's shift due to interface roughness. The light hole (lh) states, on the other hand, are unoccupied (or have a small occupancy) also at the band extremum under our conditions, which in turn results in formation of light-hole excitons from electrons and holes only with momentum close to zero. Thus there is no blueshift of the electron–light-hole exciton peaks in the PLE relative to the PL (besides the Stoke's shift) in our case. We calculate the energy of all these states in two steps. In the first step, a self-consistent Hartree calculation[5] is performed, neglecting many-body effects. In the second step, we add the many-body effects.

II. THEORY

We have determined the hole subband dispersions by a self-consistent calculation with the Schrödinger and Poisson equations. The kinetic-energy operator is given by the Luttinger-Kohn Hamiltonian,[6] which includes the interaction between the heavy holes and the light holes. It is in general a 4×4 matrix but can be decoupled into two 2×2 matrices,[7]

$$\begin{bmatrix} A_+ & C\mp iB \\ C^*\pm iB & A_- \end{bmatrix}, \tag{1a}$$

where

$$A_\pm = -\frac{\hbar^2}{2m_0}\left[(\gamma_1\pm\gamma_2)(k_x^2+k_y^2)+\left(\gamma_1\mp\frac{2\gamma_2}{\gamma_1}\right)k_z^2\right],$$

$$B=\frac{\hbar^2}{2m_0}[2\sqrt{3}\gamma_3(k_xk_z-ik_yk_z)],$$

$$C=\frac{\hbar^2}{2m_0}\left[-\sqrt{3}\,\gamma_2(k_z^2-k_y^2)-2\sqrt{3}\,\gamma_3 i k_x k_y\right]. \qquad (1b)$$

We have applied the axial approximation[5] in which an average dispersion in the xy plane is assumed. This corresponds to replacing γ_2 and γ_3 in term C in the matrix above by $(\gamma_2+\gamma_3)/2$. For the symmetric potential in this problem, both matrices give the same subband structure corresponding to a twofold spin degeneracy. Current-conserving boundary conditions are fulfilled with the use of a modified variational method described elsewhere.[8] The calculations are performed for a series of hole concentrations. In all cases considered here, only the uppermost $(n=1)$ heavy-hole subband (hh1) is found to have an equilibrium population of holes. The effect of nonparabolicity is included.[9]

The many-body effects in a QW can be incorporated in different ways. One way is to add an effective exchange-correlation potential to the Hartree potential used in the self-consistent solution of the Schrödinger-Poisson equations. This many-body potential depends on the local three-dimensional density of carriers and is the same for the different sublevels. Inclusion of this potential leads to a very small change in the dispersion of the bands and the sublevels are shifted more or less rigidly. In the present work, the change in dispersion with increasing carrier concentration is important and therefore this approach is not so useful. Besides, the local exchange-correlation potential is obtained for neutral systems and the QW is locally not neutral, since there is a space separation in the z direction between the dopant charges and the neutralizing carriers. This leads to an uncertainty as to whether the use of a local exchange-correlation potential can be applied in the QW calculations.[10] Another way to incorporate the many-body shifts is to treat the Hartree contribution and the contribution from carrier-carrier scattering on an equal footing and calculate the energy shifts in perturbation theory, as was done in Ref. 10.

We follow a third path. We first solve the Hartree problem and then use this solution as basis for a perturbation expansion where the electron-electron interaction is the perturbation. One important difference between center-doped QW's and δ-doped bulk structures is that the separation between the sublevels is much larger in the QW case. The system is here closer to a strict 2D system. The interband transitions are less important. If one neglects these interband transitions the system behaves, in principle, like a 2D system. The only difference is the matrix elements for the scattering processes, which are modified due to the finite extension of the carrier wave functions in the z direction. This modification is negligible for processes with small momentum transfers. The important contributions to the many-body effects originate from scattering processes with momentum transfers smaller than two times the Fermi momentum. Thus, for a fixed well width, there is an upper limit in the carrier concentration for the validity of a strict 2D treatment of the problem. A more narrow well pushes this limit towards higher concentrations. In our case the estimated upper limit of the carrier concentration for a strict 2D treatment is approximately 6×10^{11} cm^{-2}, which corresponds to an acceptor concentration of 2×10^{18} cm^{-3} in the doping sheet. For higher concentrations, the strict 2D treatment overestimates the many-body shifts.

In the calculations of the self-energy shifts, we neglect interband transitions. With these approximations we can treat the carriers as three different particles, electrons, heavy holes, and light holes, respectively. These particles move in a gas of heavy holes. In this part of the calculation, we also neglect nonparabolicities in the dispersion of the bands. This means that the electrons, heavy holes, and light holes are characterized by the effective masses, m_e, $m_{\rm hh}$, and $m_{\rm lh}$, respectively. Due to the Fermion statistics and the repulsion between each pair of heavy holes, a heavy hole is surrounded by an exchange-correlation hole. This exchange-correlation hole is negatively charged while the heavy hole is positively charged. The interaction between these charged species leads to a negative energy contribution for the heavy hole—a self-energy shift. The exchange-correlation hole always contains one unit of charge but its shape, and hence the size of the self-energy shift, depends on the state of the heavy hole. A light hole is surrounded by a correlation hole due to the repulsion between light holes and heavy holes. There is no exchange contribution in this case. The interaction between the correlation hole and the light hole also leads to a negative energy shift for the light hole. An electron is surrounded by an enhancement of the heavy-hole concentration due to the electron–heavy-hole attraction, which results in a negative shift of the electron energy. Thus all three types of particles attain negative energy shifts due to the interaction with the gas of heavy holes.

A similar energy shift is obtained from the interaction with the acceptors. Both types of holes are attracted by the ions and stay close to them. The electrons, on the other hand, are repelled by the ions and tend to avoid them. This leads to a reduction of the energy for all types of carriers. We neglect the effects from these carrier-impurity interactions on the exciton energy. Since the exciton is neutral, this interaction is of short-range character and should have only a minor effect on the FE. The major difference, in this respect, between the particle interaction with the heavy hole and the ion is that the latter is fixed in position.

The many-body shifts are derived in a 2D approximation, performed in a pure random-phase approximation (RPA) with Hubbard's local field correction. It turns out that the inclusion of a local field correction has only minor effects on the results. The results we present here are those with the local-field correction included. The many-body effects are derived within the Rayleigh-Schrödinger perturbation theory, or on-the-mass-shell perturbation theory.[11] In this theory, the single-particle energy for a state $(\mathbf{k},i)$ is defined as the variational derivative of the total energy with respect to the occupation number for state $(\mathbf{k},i)$, i.e.,

$$\varepsilon_{k,i}=\frac{\delta(E_{\rm tot})}{\delta n_k^i}=\varepsilon_{k,i}^0+\hbar\Sigma_{k,i}, \qquad (2)$$

where $E_{\rm tot}$ is the total energy. The first term on the right-hand side is the unperturbed single-particle energy (the kinetic energy) and the second term is the self-energy from the interactions. The index i runs over the electrons, light holes, and heavy holes.

The total interaction energy can be written as

$$E_{\rm xc} = +i\int_0^1 \frac{d\lambda}{\lambda}\frac{1}{2}\sum_{\mathbf{q}}{}' \left\{ \int_{-\infty}^{\infty} \frac{d\omega}{2\pi}\hbar\left[\frac{1}{\varepsilon^{\lambda}(\mathbf{q},\omega)}-1\right] - \frac{(N_e+N_{\rm hh}+N_{\rm lh})\lambda v_{\mathbf{q}}}{i\nu\kappa}\right\}, \tag{3}$$

where $v_{\mathbf{q}}=2\pi e^2/q$ is the 2D Fourier transform of the Coulomb potential, λ is the coupling constant for the interaction, ε is the dielectric constant for GaAs, and v is the volume of the system, respectively. The total number of carriers of type i is represented by N_i. The dielectric function in Eq. (3) is the test-particle function, i.e.,

$$\varepsilon^{\lambda}(\mathbf{q},\omega) = 1+\lambda\alpha_{0,e}(\mathbf{q},\omega)+\lambda\alpha_{0,\rm lh}(\mathbf{q},\omega) + \frac{\lambda\alpha_{0,\rm th}(\mathbf{q},\omega)}{1-f_H(\mathbf{q})\lambda\alpha_{0,\rm hh}(\mathbf{q},\omega)}. \tag{4}$$

The polarizabilities α for the light holes and electrons are included in such a way that the variational derivative with respect to the occupation numbers for these particles will produce the corresponding self-energy shifts. When the derivation has been performed, these polarizabilities can be set equal to zero. The polarizabilities are the 2D RPA functions. We have used Hubbard's local-field correction, which in 2D is given by

$$f_H(\mathbf{q}) = \frac{1}{2}\sqrt{\frac{q^2}{q^2+k_{F,\rm hh}^2}}. \tag{5}$$

A pure RPA is obtained when this function is set equal to zero.

III. SAMPLES AND EXPERIMENTAL TECHNIQUES

The samples used in this work were grown by molecular-beam epitaxy at a temperature of nominally 680 °C without interruptions at the QW interfaces. The layers were grown on a semi-insulating GaAs(100) substrate with a 0.35-μm undoped GaAs buffer layer. The $Al_xGa_{1-x}As$ barriers were 150 Å wide with $x=0.3$. The wells had a width of 150 Å and were doped with Be in the central 20% at doping levels varying from 3×10^{16} up to 1×10^{19} cm^{-3}. The Stoke's shift caused by the interface roughness is small ($\approx$0.5 meV) in the series of samples used. The hole concentrations in the QW structures were obtained by Hall measurements.

For the PL and PLE measurements, an Ar^+ ion laser was used to pump a tuneable titanium-doped sapphire solid-state laser. The emitted light from the samples was focused on the slits of a 1-m double-grating monochromator and detected with a dry-ice cooled GaAs photomultiplier. All optical measurements presented here were performed at 2 K.

IV. RESULTS AND DISCUSSION

Figure 1 displays the development of the PL spectra with increasing acceptor concentration. As can be seen, the excitonic peaks, the acceptor bound exciton (BE) and the FE_{hh} are redshifted as the acceptor concentration increases. Also, the BE gains intensity versus the FE_{hh} with increasing acceptor concentration due to the increasing probability for a FE to become trapped at an acceptor. In addition, a second BE component emerges from the ''conventional'' BE at higher doping levels. This second component has been interpreted as an exciton bound at interacting acceptors instead of the exciton bound at the single acceptor as is the case for the ''conventional'' BE.[12] This occurs when the average distance between the acceptors becomes comparable to or smaller than the extension of the exciton wave function. At higher acceptor concentrations (above $\approx2\times10^{18}$ cm^{-3}), the BE peak start to overlap with the GaAs emissions. For the same acceptor concentration, also a weak feature originating from the light-hole related exciton, FE_{lh}, can be seen in PL already at lowest temperatures,[13] reflecting the fact that the Fermi level is approaching the light-hole subband. The energy spacing between the heavy-hole recombination at the Fermi energy and the FE_{lh} has decreased to $\approx$4 meV due to filling of the hh subband.

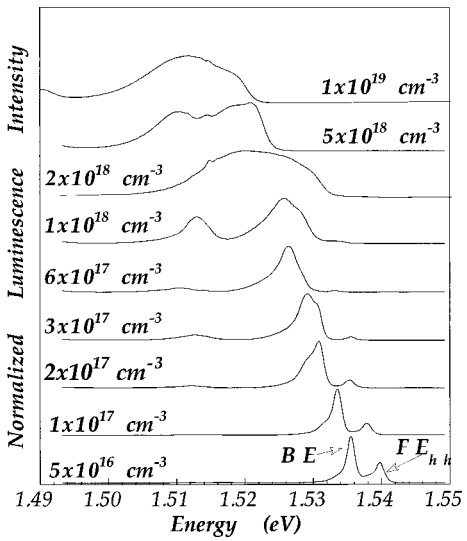

FIG. 1. PL spectra at different doping concentrations. All spectra are normalized. The acceptor bound excitons dominate even at low doping concentrations. The FE_{hh} intensity decreases continuously with increasing doping.

Figure 2 shows PLE spectra for three samples with dop-

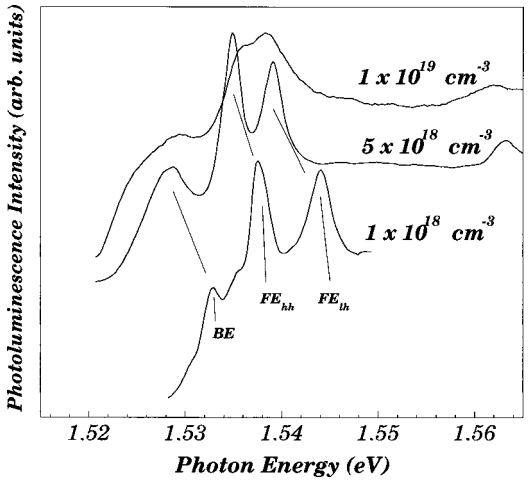

FIG. 2. PLE spectra for QW's with doping level above the degenerate limit ($\approx1\times10^{18}$ cm^{-3}): 1×10^{18}, 5×10^{18}, and 1×10^{19} cm^{-3}, respectively. Excitons are clearly seen even for the highest doping concentration shown.

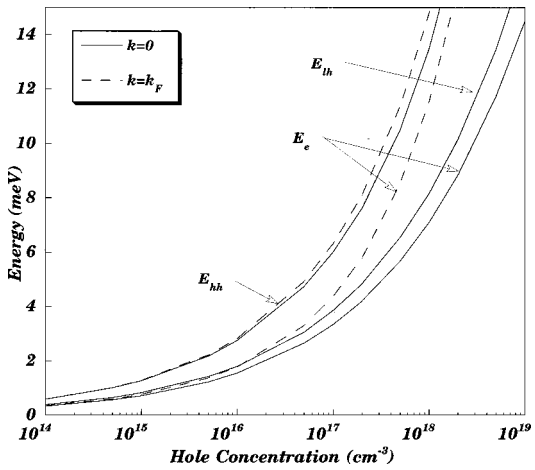

FIG. 3. Theoretically predicted renormalization of electron, heavy-hole, and light-hole subbands with the hole concentration at the bottom of the band ($k=0$) together with the corresponding dependencies of the electron and heavy-hole subbands at the Fermi wave vector (k_F) are shown in the figure.

ing concentrations above the degenerate limit ($\approx 1 \times 10^{18}$ cm^{-3}). The degenerate limit for these QW's has been determined by using the classical Hall effect in the dark. According to a procedure described in an earlier work,[14] we concluded that the sample exhibited ''metallic'' character and the hole gas was degenerate, if no dependence of the Hall concentration on the temperature was exhibited in the interval from helium temperature up to room temperature. Three distinct peaks are observed: The acceptor BE, FE_{hh}, and FE_{lh}, respectively. Even though the doping concentration is well above the degenerate limit, the excitons are still observed also at the highest doping level shown. As for *n*-type QW's,[3] the presence of excitons at such a high doping concentration is mainly due to the inefficiency of screening in a 2D system.[12] The light-hole band is normally empty at low temperatures for moderately doped samples, but as described above, for the degenerate sample, (a concentration of 2×10^{18} cm^{-3}) the FE_{lh} is observable also in PL,[13] which in turn implies that the Fermi level is approaching the light-hole band.

The exciton binding energy is assumed to be constant. According to our experimental data (PLE), the binding energy is approximately constant for doping levels up to at least 5×10^{17} cm^{-3}. The band-gap renormalization dependence, however, is sensitive to the hole concentration and exhibits a strong dependence. This is clearly illustrated in Fig. 3, where the theoretically predicted dependencies of the electron, light-hole, and heavy-hole subbands shift with the hole concentration at the bottom of the band ($k=0$) and at the Fermi wave vector (k_F) are shown. The renormalization effects for the light-hole and heavy-hole bands are different, with a stronger effect for the heavy-hole band. Furthermore, the subband shifts at $k=0$ and at the Fermi level ($k=k_F$) are significantly different for the electrons, while the corresponding difference for the heavy-hole subband is quite small. This effect contributes to a different band-gap shift deduced from PL and PLE data, respectively.

In Fig. 4, the theoretically predicted energy position of the FE's is plotted as a function of the hole concentration. The

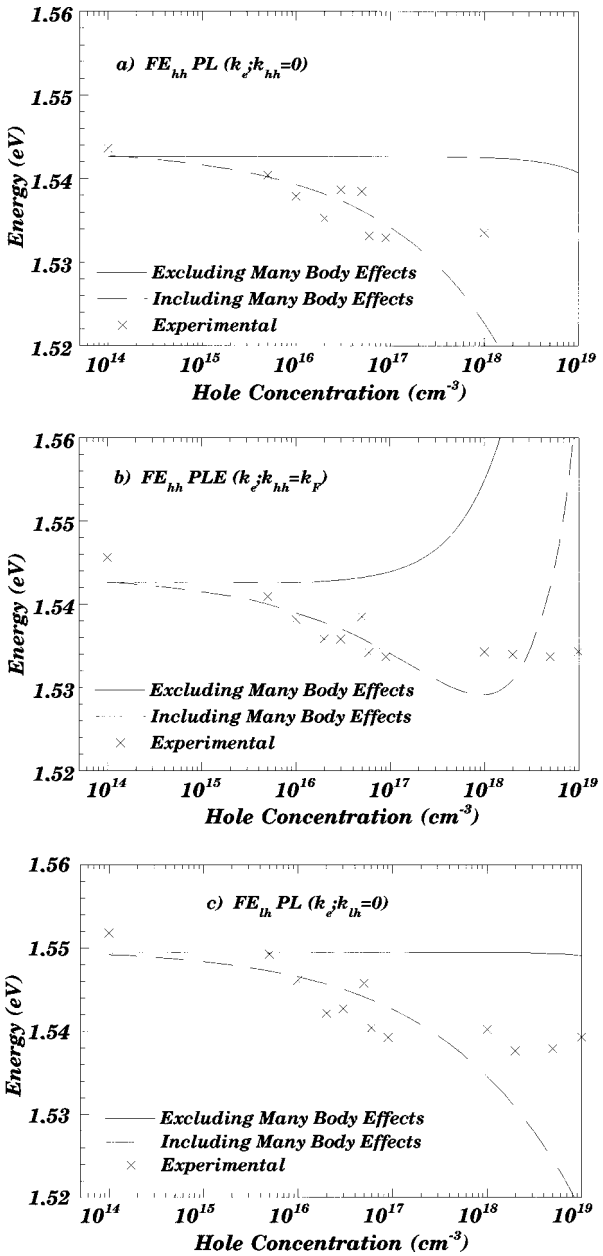

FIG. 4. Peak position dependencies of the FE's on the hole concentration for (a) FE_{hh} in PL, (b) the FE_{hh} in PLE, and (c) FE_{lh} in PLE.

effect of many-body interaction is illustrated. In the first graph, only the phase-space filling is taken into account, disregarding any many-body effect, while both phase-space filling and many-body effects are included in the second graph, as described above. Here, the FE_{hh} and FE_{lh} at the bottom of the band (i.e., $k_e=k_{hh}=k_{lh}=0$), have the same dependence on the hole concentration. In Fig. 4, our theoretical predictions are compared with experimental results achieved for the dependence of the FE energy position on the hole concentration. By comparing the effect excluding and including many-body interaction, respectively, we can conclude that many-body effects are important already at low hole concentrations, where a commencement of a deviation between the two graphs is observed.

It should be kept in mind that this theoretical model still involves significant approximations, which might not be ad-

equate in the high hole concentration regime. For the heavy-hole band, the actual dispersion curve becomes flatter for higher momentum. The many-body effects become increasingly important with increasing effective mass. Thus the neglect of nonparabolicity effects underestimates the many-body effects for high hole concentrations. Also, the 2D approximation does not hold for hole concentrations exceeding 2×10^{18} cm^{-3}. Another complication is that the chemical potential approaches the light-hole band edge. This means that intersubband transitions can no longer be neglected. It also implies that holes start to occupy the light-hole band and that the increase in k_F with density is reduced. This may explain the fact that the experimental results in Fig. 4(b) are not blueshifted for high densities.

V. SUMMARY

A combined experimental and theoretical study on acceptor-doped QW's up to concentration levels well above the degenerate limit is presented. It is concluded that many-body effects including exchange and correlation provide a first-order correction to the exciton energy already at moderate doping levels in the acceptor center-doped QW structures. Excitons are found up to a hole density of 10^{19} cm^{-3}. The theoretical approximations used are estimated to be valid for densities up to around 2×10^{18} cm^{-3}.

ACKNOWLEDGMENT

A.C.F. gratefully acknowledges financial support from RHAE/CNPq, Brazil.

[1] G. W. W. Bauer, Phys. Rev. B **45**, 9153 (1992).
[2] J. Shah, R. F. Leheny, and W. Wiegmann, Phys. Rev. B **16**, 1577 (1977).
[3] C. I. Harris, B. Monemar, H. Kalt, and K. Köhler, Phys. Rev. B **48**, 4687 (1993).
[4] S. Schmitt-Rink, D. S. Chemla, and D. A. B. Miller, Adv. Phys. **38**, 89 (1989).
[5] U. Ekenberg and M. Altarelli, Phys. Rev. B **32**, 3712 (1985).
[6] J. M. Luttinger and W. Kohn, Phys. Rev. **97**, 869 (1955); J. M. Luttinger, *ibid.* **102**, 1030 (1956).
[7] D. A. Broido and L. J. Sham, Phys. Rev. B **31**, 888 (1985).
[8] M. Altarelli, Phys. Rev. B **28**, 842 (1983).
[9] U. Ekenberg, Phys. Rev. B **40**, 7714 (1989).
[10] O. Betbeder-Matibet, M. Combescot, and C. Tanguy, Phys. Rev. Lett. **72**, 4125 (1994).
[11] T. M. Rice, Ann. Phys. (Leipzig) **31**, 100 (1965).
[12] A. C. Ferreira, P. O. Holtz, B. E. Sernelius, I. Buyanova, B. Monemar, O. Mauritz, U. Ekenberg, M. Sundaram, J. L. Merz, and A. C. Gossard, Phys. Rev. B **54**, 16 989 (1996).
[13] A. C. Ferreira, P. O. Holtz, B. Monemar, M. Sundaram, K. Campman, J. L. Merz, and A. C. Gossard, Phys. Rev. B **54**, 16 994 (1996).
[14] A. Buyanov, A. C. Ferreira, E. Söderström, I. A. Buyanova, P. O. Holtz, B. Sernelius, B. Monemar, M. Sundaram, K. Campman, J. L. Merz, and A. C. Gossard, Phys. Rev. B **53**, 1357 (1996).